

Doppler shifted cyclotron resonance and electromagnetic waves in copper

V. V. Lavrova, C. V. Medvedev, V. G. Skobov, L. M. Fisher, A. S. Chernov, and V. A. Yudin

All-Union Electro-technical Institute

A. F. Ioffe Physico-technical Institute, USSR Academy of Sciences

(Submitted July 17, 1973)

Zh. Eksp. Teor. Fiz. 66, 700-713 (February 1974)

The Doppler shifted cyclotron resonance in copper in the presence of an applied magnetic field parallel to the [110] axis has been investigated both theoretically and experimentally at radio frequencies. The theoretical treatment is based on a model Fermi surface having rotational symmetry. It is shown that the resonance of the electrons undergoing minimal displacement during a cyclotron period leads to the propagation of a weakly damped, circularly polarized electromagnetic wave, the doppleron, whose circular polarization is opposite in sense to that of the helicon. The wavelength of the doppleron is close to the minimal electron displacement, so the excitation of dopplerons results in impedance oscillations with a period close to that of the Gantmakher-Kaner oscillations. The oscillations in the derivative of the surface resistance of a copper plate as a function of the strength of an applied magnetic field perpendicular to the surface were investigated experimentally, a circularly polarized rf field being used for excitation. The experimental results concerning the polarization of the impedance oscillations and the dispersion of their period are in full agreement with theory. This proves that the oscillations are not a manifestation of the Gantmakher-Kaner effect, but are actually due to doppleron excitation.

1. INTRODUCTION

The Doppler-shifted cyclotron resonance (DSCR) is associated with the Fermi statistics of the conduction electrons and is characteristic of metals. One of its consequences is that the range of magnetic field strengths in which helicons exist is bounded from below.^[1] Another physical consequence of the DSCR is the rf size effect in a normal magnetic field^[2]. The presence of a collisionless-absorption edge leads to the appearance of a branch point in the functional dependence of the nonlocal conductivity on the wave vector k , and this in turn leads to the existence of a small penetrating component of the rf field. The phase of this component increases linearly with the magnetic field strength H , so that the impedance of the plate undergoes periodic oscillations—the Gantmakher-Kaner (GK) effect. This component is not an eigenmode of the electromagnetic field in the electron plasma of the metal, but its wave vector is a solution of the dispersion equation. Its amplitude decreases inversely as the square of the distance from the surface, and as a result the amplitude of the GK oscillations is proportional to the small parameter $(\delta/d)^2$, where δ is the depth of the anomalous skin layer and d is the thickness of the plate. Characteristic features of the GK oscillations are 1) a constant period, 2) a low amplitude, which is independent of the magnetic field strength in the anomalous skin effect region, and 3) linear polarization.

Finally, the presence of a cyclotron-absorption edge indicates dispersion of the dielectric constant of the electron gas and may lead to the appearance of new solutions to the dispersion equation describing propagating modes.^[3,4] In alkali metals in a transverse magnetic field, the DSCR is due to electrons of the limiting point, which have a large longitudinal velocity and no transverse velocity and therefore make only a small contribution to the transverse conductivity. At the same time, the electrons lying close to the central cross section of the Fermi surface have small longitudinal velocities and make a large local contribution to the transverse conductivity. As a result, the singularity of the nonlocal conductivity in the DSCR region is weak, and there is virtually no resonance mode (doppleron).

The DSCR in metals having an anisotropic Fermi surface can be considerably stronger. It was shown in^[5] that in cadmium the DSCR leads to strong dispersion of the nonlocal conductivity and to the possible propagation of a electronic- and hole-type dopplerons. In this case the DSCR due to the electrons at the limiting point of the lens is strong because the contribution to the Hall conductivity from nonresonance electrons is almost entirely compensated by the hole contribution. The wavelength of the electronic doppleron is somewhat greater than the maximum displacement of the electrons during a cyclotron period. Hence the excitation of waves in the plate leads to impedance oscillations which at first glance seem similar to GK oscillations but are actually quite different from them. First, the period of the cadmium impedance oscillations varies appreciably with the magnetic field; second, there is a sharp magnetic-field threshold below which the oscillations are not observed, whereas the amplitude of GK oscillations should remain virtually constant; and third, the amplitude of the observed oscillations is large, being comparable with the amplitude of helicon oscillations in uncompensated metals. The amplitude of these oscillations does not contain the small parameter $(\delta/d)^2$ and is several orders of magnitude larger than the amplitude of GK oscillations. All these characteristics of the observed oscillations find a natural explanation in terms of resonance waves-dopplerons.^[5] It also follows from the theory that the doppleron, unlike GK oscillations, is circularly polarized, its field rotating in the same sense as the electrons. It was shown experimentally in^[6] that cadmium impedance oscillations are actually observed only when the exciting field is circularly polarized in the appropriate sense.

The possibility of making a quantitative comparison between theory and experiment for cadmium is due to the fact that the electron lens has a fairly simple shape and can be easily described mathematically. At the same time the holes of the monster have considerably smaller displacements, and a good description of their contribution to the conductivity is obtained in the local approximation, in which the complex shape of the monster is not involved. The Fermi surfaces of other

anisotropic metals are more complex, and for them one cannot calculate the nonlocal conductivity in analytic form. In particular, this is the case for copper, which is the first metal in which variations in the period of the impedance oscillations were detected^[7]. The simple models of anisotropic Fermi surfaces proposed in^[8,9] for approximate calculations of DSCR cannot account for all the characteristics of the oscillations observed in copper, while the numerical calculations published in^[10,11], which were based on a more complicated model, do not enable one to understand the physical nature of the oscillations.

Here we report the results of a theoretical and experimental study of surface-resistance oscillations of a copper plate for the case in which the normal n to the surface and the magnetic field H are parallel to the twofold axis [110]. A model that correctly describes the characteristic features of the Fermi surface of copper was used in the calculations. Using this model, one obtains a simple analytic expression for the nonlocal conductivity, and the resulting dispersion equation can be analyzed. It is shown that the DSCR of electrons having minimal displacement along the field leads to the existence of a doppleron whose circular polarization is opposite in sense to that of a helicon. The surface resistance of a copper plate was measured experimentally for circularly polarized exciting fields. Impedance oscillations with a period corresponding to the minimum value of the derivative to the cross sectional area of the Fermi surface were observed only when the circular polarization of the exciting field was "positive," i.e., opposite to that of a helicon. The oscillations exist over a wide range of magnetic field strengths, both above and below the helicon threshold. The period of the oscillations is not constant but, in agreement with the results of the theoretical calculation, varies by 40%.

2. THEORY

A. Fermi Surface Model

The properties of the doppleron are determined by the behavior of the nonlocal conductivity in the vicinity of the DSCR, and the behavior of the conductivity is determined, in turn, by the shape and topology of the Fermi surface. The relation between the nonlocal conductivity and the shape of the Fermi surface is very complicated for the case of arbitrary orientations of the wave vector k and the magnetic field H , but it simplifies considerably if the Fermi surface has rotational symmetry and the vectors k and H are parallel to this rotational symmetry axis. In the latter case the conductivity can be written in the form

$$\sigma_{\pm}(k, H) = \sigma_{xx} \pm i\sigma_{yx} \quad (1)$$

$$= \pm i \frac{ec}{H} \frac{2}{(2\pi\hbar)^3} \int dp_z S(p_z) \left(1 - \frac{kc}{2\pi eH} \frac{\partial S}{\partial p_z} \pm i\gamma \right)^{-1},$$

where

$$\gamma = \frac{vc}{2\pi eH} \frac{\partial S}{\partial e_F}, \quad (2)$$

e is the magnitude of the electron charge, c is the velocity of light, ν is the carrier-lattice collision frequency, and $S(\epsilon_F, p_z)$ is the area of the cross section of the Fermi surface $\epsilon(p) = \epsilon_F$ cut by the plane $p_z = \text{const}$ perpendicular to the magnetic field H (S is positive for electron orbits and negative for hole orbits). The expression σ_{\pm} for the conductivity corresponds to the case of a wave whose electric vector rotates clock-

wise in the xy plane ("positive" circular polarization), and the expression σ_{-} , to the case of a wave whose electric vector rotates counterclockwise ("negative" circular polarization).

In the local collisionless limit, the denominator of the integrand in (1) reduces to unity and σ_{\pm} reduces to the static Hall conductivity. The second term in the denominator plays an important part under nonlocal conditions: the integrand has an anomaly at

$$\frac{2\pi}{k} = u(p_z) = -\frac{c}{eH} \frac{\partial S}{\partial p_z}, \quad (3)$$

where u is the mean displacement of the carriers during a cyclotron period. Electrons with different values of p_z resonate at different values of k/H . Hence the integration over p_z weakens the resonance so that $\sigma(k)$ has a resonance-type anomaly only for values of $2\pi/k$ equal to the extremal displacement u_{ext} of the carriers. The nature of the anomaly depends on the behavior of the function $S(p_z)$ and its derivative $\partial S/\partial p_z$ in the p_z region in which the derivative has its extremum. The anomaly will be a singularity if the resonant electrons have orbits of finite size ($S \neq 0$) and will be weak if the resonance is due to electrons at an elliptic limiting point ($S = 0$). The anomalies of the nonlocal conductivity for various model Fermi surfaces are discussed in^[1-6,8-11].

The Fermi surface of copper is well known; it is highly anisotropic and its cross section area $S(p_z)$ is a complicated function of p_z . P. L. Powell has made numerical calculations of the Fermi surface (see^[12]) and the graphs of $S(p_z)$ and $\partial S/\partial p_z$ as functions of p_z are given in^[12] for the three principal crystallographic directions. These graphs for the case $H \parallel [110]$ are shown in Fig. 1 by thin lines. Closed hole orbits of "dog bone" type occur in the region $|p_z| < p_1$, where $p_1 = 0.2p_F$ with $p_F = 1.36\hbar \text{ \AA}^{-1}$. The derivative $\partial S/\partial p_z$ tends to infinity as $p_z \rightarrow p_1$. This singularity is associated with the fact that the limiting orbit necessarily

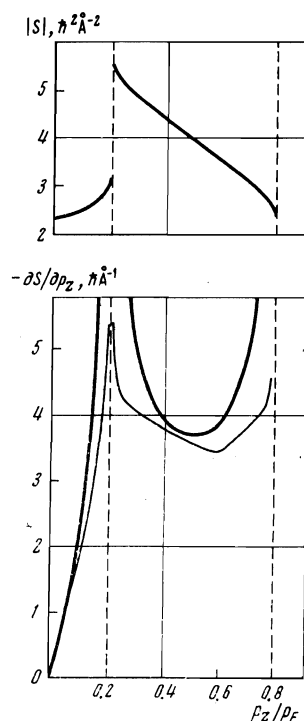


FIG. 1. Cross section area $S(p_z)$ of the Fermi surface and its derivative $\partial S/\partial p_z$ as functions of p_z for the case $p_z \parallel [110]$. The thin lines are from^[12].

passes through a saddle point on the Fermi surface, where the nature of the orbit changes radically.

There are closed electron orbits in the region $p_1 < |p_z| < p_2$, where $p_2 = 0.8p_F$, and in the region $|p_z| > p_2$ there is a layer of open orbits for which the concept of area has no meaning.

With such a complicated Fermi surface, the nonlocal conductivity can obviously be calculated only numerically. Numerical calculations of the impedance of a plate were made in^[10,11] for a model Fermi surface, and it was shown that near the helicon threshold the impedance of the plate suffers oscillations whose period corresponds to an extremal value of $\partial S/\partial p_z$. Unfortunately, these calculations shed little light on the physical nature of the oscillations. The observed oscillations were interpreted in^[10] as a result of the interaction of a damped helicon with a GK wave, and the impedance oscillations of a copper plate were interpreted in a similar manner in^[12,13].

We do not agree with this interpretation; we feel that the observed oscillations are due to the excitation of a DSCR mode (i.e., a doppleron). In what follows we shall demonstrate the correctness of our view on the basis of a model that gives a qualitatively correct description of the variations of S with p_z but is still simple enough to permit one to calculate the conductivity in analytic form and to describe the properties of the doppleron and the impedance oscillations associated with it.

We shall consider a model in which the cross-section areas of the axially symmetric Fermi surfaces for electrons and holes are given as functions of p_z by the expressions

$$S_h(p_z) = -S_1 \left[\alpha - \sqrt{1 - \left(\frac{p_z}{p_1}\right)^2} \right], \quad |p_z| < p_1; \quad (4)$$

$$S_e(p_z) = S_0 - \pi p_0 (p_z - p_1) \arcsin \left(\frac{2|p_z| - p_2 - p_1}{p_2 - p_1} \right), \quad (5)$$

$$p_1 < |p_z| < p_2;$$

here α , p_0 , S_0 , and S_1 are constants.

The graphs of the functions $S_h(p_z)$ and $S_e(p_z)$ for the parameter values

$$\alpha = 3.3, \quad p_0 = 0.59\hbar \text{ \AA}^{-1}, \quad S_0 = 4S_1 = 4\hbar^2 \text{ \AA}^{-2} \quad (6)$$

are virtually the same as the corresponding graphs resulting from Powell's calculation^[12] and shown in the upper part of Fig. 1. The graphs of $\partial S_h/\partial p_z$ and $\partial S_e/\partial p_z$ are shown by the heavy curves in the lower part of Fig. 1; they differ considerably from the thin curves (taken from^[12]) but behave in a qualitatively similar manner. The minimum value of $\partial S_e/\partial p_z$ is $2\pi p_0$, and this quantity determines the period of the impedance oscillations in strong fields. We chose the value of p_0 so as to make the theoretical value of this period equal to the observed period.

B. Nonlocal Conductivity and the Dispersion Equation

Now let us calculate the nonlocal conductivity on the basis of our model. To do this we substitute expressions (4) and (5) for $S(p_z)$ into Eq. (1) and integrate over p_z from $-p_2$ to $+p_2$, regarding γ as constant. The result can be written in the form

$$\sigma_{\pm}(q) = \pm i \frac{ec}{H} \left[\frac{N_e}{1 \pm i\gamma_e} F\left(\frac{q}{1 \pm i\gamma_e}\right) - \frac{N_h}{1 \mp i\gamma_h} J\left(\frac{\eta q}{1 \mp i\gamma_h}\right) \right], \quad (7)$$

$$F(q) = 1 - \frac{q^2}{\sqrt{1-q^2}} \operatorname{arctg} \frac{1}{\sqrt{1-q^2}}, \quad (8)$$

$$J(x) = \frac{1}{1+x^2} \left(1 - \frac{\pi}{4\alpha} \right)^{-1} \left[1 - \frac{\pi}{4\alpha} - \frac{\pi x^2 (1 - \sqrt{1-x^2})}{2(1+x^2)} + \frac{\alpha x^2}{2\sqrt{1+x^2}} \ln \frac{1 + \sqrt{1+x^2}}{1 - \sqrt{1+x^2}} \right], \quad (9)$$

where

$$q = \frac{kc p_0}{eH}, \quad \eta = \frac{S_1}{2\pi p_1 p_0}, \quad (10)$$

$$N_e = \frac{4S_0(p_2 - p_1)}{(2\pi\hbar)^3}, \quad N_h = \frac{4S_1 p_1}{(2\pi\hbar)^3} \left(\alpha - \frac{\pi}{4} \right). \quad (11)$$

N_e and N_h are the electron and hole concentrations, q is the ratio of the minimum electron displacement during a cyclotron period to the wavelength of the electromagnetic wave, and γ_e and γ_h characterize the scattering of electrons and holes. In the following we shall consider the case of infinite carrier mean free path: $\gamma_e = \gamma_h = 0$.

The functions $F(q)$ and $J(\eta q)$ describe the nonlocal effects in the conductivity. As q increases from zero, $\operatorname{Re} J$ increases smoothly, reaches a maximum in the region $\eta q \sim 1$, and then tends asymptotically to zero. When q is small, $\operatorname{Im} J$ increases quadratically from zero, remaining small as compared with $\operatorname{Re} J$. In the region $\eta q \sim 1$, the imaginary part of J is of the same order as the real part and also has a maximum, and as q increases further it tends to zero as $1/q$. The imaginary part of J is due to collisionless cyclotron absorption of the wave by holes. In the present case this absorption is finite for all finite values of q and has no threshold. In accordance with the Kramers-Kronig relations, $\operatorname{Re} J$ is also a smooth function of q with no singularities. In other words, there is no DSCR in the hole conductivity. This is due to the fact that the mean displacement of the holes during a cyclotron period, which is proportional to $\partial S/\partial p_z$, varies monotonically from $-\infty$ to $+\infty$. For comparison, we recall that in the case of a convex Fermi surface $\partial S/\partial p_z$ varies between finite limits, so that the cyclotron absorption region has a long-wavelength threshold.

Now let us consider the electronic part of the nonlocal conductivity. The imaginary part of F , which is due to cyclotron absorption of the wave by electrons, differs from zero for q in the range $0-1$. The imaginary part of F increases quadratically from zero when q is small and becomes comparable with $\operatorname{Re} F$ when $q \lesssim 1$. As q approaches unity, $\operatorname{Im} F$ becomes infinite as $(1 - q^2)^{-1/2}$. This singularity represents electronic DSCR. The condition $q = 1$ means that the minimum displacement of the electrons during a cyclotron period is equal to the wavelength of the electromagnetic wave. When $q > 1$ the expression under the radical sign in (8) is positive, F is real, and there is no collisionless absorption. Thus, cyclotron absorption of the wave by electrons takes place in the long-wavelength region in which $q < 1$ but not in the short-wavelength region in which $q > 1$. This situation is opposite to that which obtains for metals that have a convex Fermi surface. The physical reason for this difference is simple: In metals with a convex Fermi surface, $|\partial S/\partial p_z|$ ranges from zero to some finite value and condition (3) for cyclotron absorption is satisfied only for fairly large values of k , whereas in our case $\partial S/\partial p_z$ varies from some minimum value to infinity, so that collisionless absorption takes place only for small q .

When q is small, the real part of F is large compared with $\operatorname{Im} F$, which is proportional to q^2 in this

region. In the region $q \lesssim 1$, $\text{Re } F$ varies smoothly, remaining positive, while $\text{Im } F$ is of the order of unity. In other words, the nonlocal conductivity is essentially complex when $q \lesssim 1$. At $q = 1$, $\text{Re } F$ has an infinite discontinuity and changes sign, and for large q it tends monotonically to zero, remaining negative. This dispersion of $\text{Re } F$ in the region $q > 1$ is due to DSCR of electrons, which leads to a root singularity in $\sigma(q)$. In this case, $\text{Im } F$ becomes infinite to the left of the point $q = 1$, and $\text{Re } F$, to the right of it, as is typical for root singularities.

There are not only closed electron and hole orbits in copper when $\mathbf{H} \parallel [110]$, but there is also a layer of open orbits in the region $|p_z| > p_z$. The concentration N_0 of carriers with open orbits is roughly equal to $0.04N_e$ when \mathbf{H} is strictly parallel to the $[110]$ axis. The open orbits disappear when the magnetic field deviates from the $[110]$ axis by an angle $\chi_0 = 2^\circ$. The transverse conductivity due to carriers with open orbits has the same form as in the local limit in the absence of a magnetic field. This conductivity can be approximated by the expression

$$\sigma_0 = \frac{N_0 e^2}{m\nu} \left(1 - \frac{\chi}{\chi_0}\right) \theta(\chi_0 - \chi), \quad (12)$$

where χ is the angle between \mathbf{H} and the $[110]$ axis, while $\theta(x) = 1$ for positive x and $\theta(x) = 0$ for negative x .

The open-orbit transverse conductivity (12) is proportional to the free flight time $1/\nu$ of the carriers, so it can be comparable with $\text{Im } \sigma_{\pm}$, despite the relatively small number of open orbits. This results in strong damping of the helicon when $\mathbf{H} \parallel [110]$. When \mathbf{H} deviates from the $[110]$ axis by the angle $\chi_0 = 2^\circ$ the open orbits disappear, the conductivity given by (12) vanishes, and the helicon is weakly damped^[10, 12, 13]. In what follows we shall be mainly interested in the electronic DSCR region where $|\sigma_{\pm}| \gg \sigma_0$.

The dispersion equation for a circularly polarized wave in the case under consideration has the form

$$k^2 c^2 = 4\pi i \omega [\sigma_{\pm}(q) + 1/2 \sigma_0], \quad (13)$$

where ω is the frequency of the wave. Substituting (7), (8), and (12) into (13) and using the dimensionless variable q in place of k , we obtain

$$\Phi_{\pm}(q) = \omega_L / \omega, \quad (14)$$

$$\Phi_{\pm}(q) = \frac{1}{q^2} \left\{ \pm \left[F(q) - \frac{N_h}{N_e} J(\eta q) \right] + i \frac{N_0}{2\gamma N_e} \left(1 - \frac{\chi}{\chi_0}\right) \theta(\chi_0 - \chi) \right\} \quad (15)$$

$$\omega_L = \pi^2 \hbar^2 e H^3 / 2 S_0 (p_2 - p_1) p_0^2 c. \quad (16)$$

We note that the signs of F and $\text{Im } J$ are determined by the signs of the small imaginary terms $i\gamma_e$ and $i\gamma_h$ occurring in the arguments of the functions F and J (see Eqs. (7)–(9)). These signs are such that all the terms in both $\text{Im } \Phi_{-}$ and $\text{Im } \Phi_{+}$ are positive.

C. Properties of the Helicon and Doppleron

Let us consider solutions (14) to the dispersion equation. We begin with the simplest case in which $\chi \gtrsim \chi_0$ and there are no open orbits. We are interested in solutions describing waves that propagate. Such solutions can exist only for values of q such that $\text{Im } \Phi \ll \text{Re } \Phi$. It is clear from what was said above that there are two regions of such q values. The first is the region of small q where the cyclotron absorption is small as compared with the absorption due to the static Hall

conductivity. This is the region in which the solution describing the helicon exists. The second region lies at $q \gtrsim 1$, where there is no cyclotron absorption of the wave by electrons and $\text{Re } \Phi$ increases rapidly because of the electron DSCR. The corresponding solution describes the doppleron.

The region in which the wave exists, and its spectrum, are most easily determined graphically. To do this we plot the function $\text{Re } \Phi_{-}(q)$ and draw a horizontal line corresponding to the selected value of ω_L / ω . The point of intersection of the line with the $\text{Re } \Phi_{-}$ curve gives the value of q , and hence the wavelength, for the chosen values of the magnetic field strength and frequency. Figure 2 shows graphs of $\text{Re } \Phi_{-}$ and $\text{Im } \Phi_{-}$. When q is small, F and J are close to unity, $\text{Re } \Phi_{-} \propto q^{-2}$, and $\text{Im } \Phi_{-} \sim 1$. For large values of ω_L / ω , the dispersion equation obviously has an almost real solution that describes a helicon wave with "negative" polarization. As the magnetic field strength decreases and ω_L approaches ω , the quantity q increases; then the real part of Φ_{-} falls while the imaginary part rises, so that the real and imaginary parts become of the same order of magnitude in the region $q \lesssim 1$. As a result, the solution to the dispersion equation becomes essentially complex, i.e., the helicon is strongly attenuated. Thus, the quantity ω_L , which is proportional to H^3 , represents the limiting helicon frequency for fixed field strength H .

Open orbits arise when $\chi < \chi_0$, and then the consequent dissipative conductivity greatly increases the helicon attenuation. The imaginary part of Φ_{-} is then of the order of $0.02/\gamma q^2$ and may be comparable with the real part, so that helicon propagation becomes impossible.

In the wavelength region $q > 1$, where $\text{Im } \Phi_{-}$ is small as compared with $\text{Re } \Phi_{-}$, the latter is negative, whereas $\text{Re } \Phi_{+}$, on the other hand, is positive, ranging from $+\infty$ to 0. This means that there is a solution to the dispersion equation with $q > 1$ that describes a doppleron with "positive" circular polarization. We emphasize that the circular polarization of this doppleron is opposite in sense to that of the helicon, whose field rotates in the same sense as the electrons. The

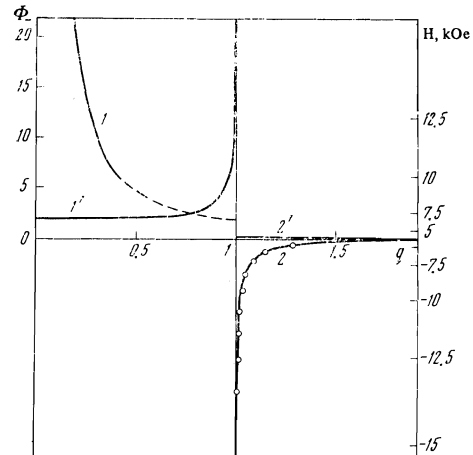


FIG. 2. Graphs of the real (curves 1 and 2) and imaginary (curves 1' and 2') parts of $\Phi(q)$. The magnetic field strength H is laid off on a cubic scale on the right-hand axis, the proportionality constant between Φ and H^3 corresponding to a frequency of 167 kHz. The points were calculated from experimental data.

reason for this is that in the present case the DSCR is due to electrons with minimal displacement, rather than to electrons with maximal displacement. In fact, when $q > 1$ the second term in the denominator of the integrand in (1) is greater than the first term, so that the sign of the resonance term in the nondissipative conductivity is opposite to that of the static Hall conductivity of the electrons. In other words, above the cyclotron absorption threshold ($q > 1$) the Doppler frequency shift exceeds the electron cyclotron frequency, and the contribution to the nonlocal conductivity from the electrons has the same sign as that from the holes. Whenever the DSCR is due to minimal displacement electrons, therefore, the doppleron field and the electrons will rotate in opposite senses. If the DSCR is due to carriers with maximal displacement, however, the doppleron field will rotate in the same sense as these carriers. That is the situation that obtains in cadmium.

The function $\Phi(q)$ changes very rapidly near the resonance, so when $\omega_L/\omega \approx 1$ the solution to the dispersion equation gives a value of q close to unity (see Fig. 2). Hence the doppleron wavelength turns out to be close to the minimal displacement of an electron during a cyclotron period. Figure 3 shows the doppleron wave number as a function of the magnetic field strength. It will be seen that the $k'(H)$ curve runs somewhat above the dashed line

$$k_0 = 2\pi/u_{\min} = eH/p_0c. \quad (17)$$

The $\Phi(q)$ curve runs less steeply in the region of large q values. Hence the k' curve rises above line (17) as H decreases.

In order to find the attenuation of the doppleron we express q in the form $q = q' + iq''$. Assuming q'' to be small as compared with $q' - 1$, we expand $\Phi_+(q)$ in powers of iq'' and, retaining only the linear term in the expansion, we separate the real and imaginary parts of the dispersion equation. As a result we obtain the following equation for the imaginary part k'' of the doppleron wave number:

$$k'' = \frac{eH}{p_0c} q'' = -\frac{eH}{p_0c} \text{Im} \Phi_+(q') \left[\frac{d}{dq'} \text{Re} \Phi_+(q') \right]^{-1}, \quad (18)$$

where $\text{Im} \Phi$ is determined by the cyclotron absorption of the wave by holes.

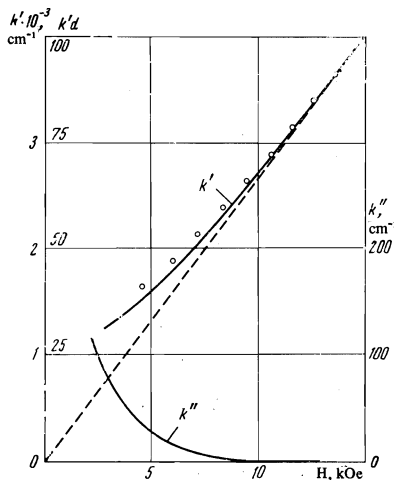


FIG. 3. Real and imaginary parts of the doppleron wave vector vs magnetic field strength for a frequency of 167 kHz. The curves were calculated; the points represent experimental data.

In the strong-field region $\omega_L > \omega$, the derivative $d\Phi/dq'$ increases without limit, and the nonlocal damping of the doppleron, as given by Eq. (18), tends to zero. Hence the part of the damping that is associated with collisions must be taken into account when H is large. The electron collisions, which give rise to the presence of the imaginary quantity $i\gamma_e$ in (7), lead to additional damping of the doppleron specified by the quantity $k_c'' = 1/l$, where $l = p_0/m\nu$ is the mean free path of the resonance electrons.

As the magnetic field strength decreases, the quantity $|d\Phi/dq'|$ decreases more rapidly than linearly, so that the damping k'' rises. Figure 3 shows the $k''(H)$ curve calculated without allowing for electron collisions; it will be seen that the attenuation becomes very great when $H \sim 3$ kOe. Hence it is difficult to observe the passage of a doppleron through the plate in weaker fields.

A doppleron is excited in the specimen when the latter is placed in an rf field having "positive" circular polarization. The phase of the signal after it has passed through the plate will be $k'd$. The quantity k' depends on the field strength H , so the impedance of the plate will be an oscillating function of H , the period of the oscillations being

$$\Delta H = (\Delta H)_{\text{GK}} [q' + 3\Phi(q') (d\Phi/dq')^{-1}]^{-1}, \quad (19)$$

where $(\Delta H)_{\text{GK}} = 2\pi p_0 c / ed$ is the period of the GK oscillations^[2].

In strong fields ($\omega_L \gg \omega$), q' tends to unity, the second term in the brackets in Eq. (19) tends to zero, and the period ΔH of the oscillations tends to the period $(\Delta H)_{\text{GK}}$ of the GK oscillations. As the magnetic field strength decreases the second term in the brackets increases, the difference between the terms in the brackets decreases, and the period ΔH increases. Figure 4 shows $\Delta H / (\Delta H)_{\text{GK}}$ as a function of H .

The presence of open orbits when $\chi < \chi_0$ has less effect on the doppleron than on the helicon. The reason for this is as follows. In strong fields ($\omega_L \gg \omega$) the doppleron branch of the function $\Phi(q)$ (curve 2 in Fig. 2) is very steep. Hence the doppleron attenuation as given by Eq. (18), which is inversely proportional to $d\Phi/dq'$, remains small despite the appearance of an additional term in $\text{Im} \Phi$. In such fields the damping of the doppleron is due as before to collisions of resonance electrons, and the damping constant is equal to $1/l$. On the other hand, the factor $1/\gamma$ in the last term on the right in Eq. (15) is appreciably smaller in weak fields ($\omega_L \ll \omega$) than it is in fields in which the helicon can exist ($\omega_L > \omega$). As a result, it turns out that the presence of open orbits leads to strong damping of the helicon but has little effect on the damping of the doppleron.

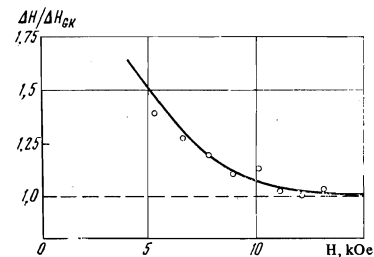


FIG. 4. Ratio of the period of the doppleron oscillations to that of the GK oscillations vs magnetic field strength. The curves were calculated; the points represent experimental data.

Thus, the theory shows that there should be both a helicon and a doppleron in copper when $k \parallel [110]$ and $\chi(H, k) \approx \chi_0$, and that these two waves should be circularly polarized in opposite senses. A linearly polarized rf field excites both waves, and when the strength of the applied magnetic field is such that both waves can exist, their interference results in a complicated pattern of oscillations^[7,10,12,13]. It should be possible to distinguish between the helicon and the doppleron by using circularly polarized exciting fields, for a circularly polarized field should excite only the wave whose electric vector rotates in the same direction as that of the exciting field. Hence we undertook an experimental study of the impedance of a copper plate, using circularly polarized exciting fields. The results of this study are presented in the following section of the paper.

3. EXPERIMENT

We investigated the surface impedance of a copper plate in a circularly polarized electromagnetic field over the frequency range from 0.13 to 3.50 MHz. Using a constant sensitivity autodyne detector, we measured the derivative dR/dH of the surface resistance as a function of the strength H of an applied magnetic field normal to the surface of the plate.

The applied magnetic field (strength up to 14 kOe) was produced by an electromagnet and was amplitude modulated at a frequency of 10 Hz. The direction of the applied field with respect to the crystallographic axes of the specimen could be adjusted by rotating the electromagnet in the horizontal plane and inclining it at angles up to 5° in two vertical planes. The symmetry of the recorded dR/dH curve served to check whether the magnetic field was strictly normal to the surface of the plate.

Two coils perpendicular to one another were used to obtain the circularly polarized rf field; one of these coils was the tank coil of the autodyne detector and the other coil was fed with an rf voltage 90° out of phase with the voltage across the autodyne tank. The sign of the circular polarization was changed by reversing the direction of the dc magnetic field. The measurement technique is described in more detail in^[7].

The plane parallel copper plates were cut from a single crystal bar^[1] by an electroerosion method. The technique used in preparing the specimens is described in detail in^[14]. The resistivity ratio $\rho(293^\circ\text{K})/\rho(4.2^\circ\text{K})$ for the specimens used in the measurements was 1.4×10^4 . The normal to the surface of the plate coincided with the $[110]$ direction within 1° . Most of the measurements were made at 4.2°K on a specimen 0.25 mm thick. Reducing the temperature to 1.5°K did not significantly increase the amplitude of the observed oscillations.

Examples of dR_{\pm}/dH curves are presented in Fig. 5. Curves 1 and 2 were recorded at $\chi = 3^\circ$, and curves 1' and 2' at $\chi = 0$; curves 1 and 1' were recorded with "negative circular polarization, and curves 2 and 2', with "positive" polarization. Curve 1 shows a few oscillations in the region $H > 8$ kOe; these oscillations are due to helicon excitation. Curve 2 exhibits a series of short period oscillations associated with doppleron excitation. These oscillations are observed in the region $H > 3$ kOe; their amplitude reaches a maximum at $H \approx 7$ kOe and decreases smoothly as H increases further. Such an H dependence of the amplitude is char-

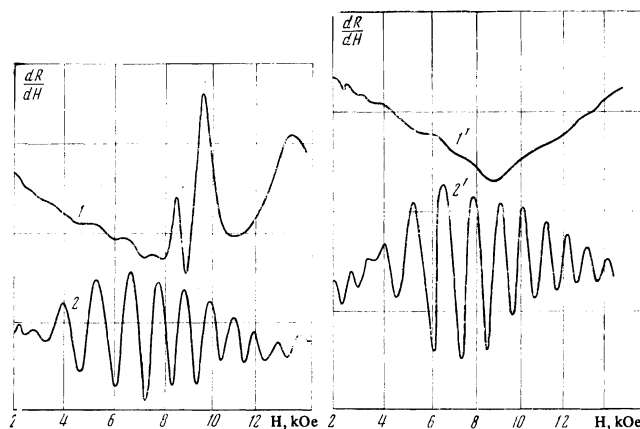


FIG. 5. Derivative dR/dH of the surface resistance of a plate measured at $\chi = 3^\circ$ (curves 1 and 2) and $\chi = 0$ (curves 1' and 2') using circularly polarized exciting fields; $\omega/2\pi = 167$ kHz, $d = 0.25$ mm, $T = 4.2^\circ\text{K}$. (Different gains were used in recording curves 1 and 2 and curves 1' and 2'.)

acteristic of doppleron oscillations^[5]. These oscillations are observed both below and above the helicon threshold, and the doppleron amplitude has no anomaly at all at that threshold. On the other hand, there are no doppleron oscillations on curve 1, which corresponds to the helicon polarization. This shows that the doppleron and helicon have opposite circular polarizations.

Curve 2' on Fig. 5, which was recorded with "positive" polarization at $\chi = 0$, hardly differs from curve 2. On the other hand, curve 1', which was recorded with "negative" polarization, shows no oscillations at all; this is due to the strong attenuation of the helicon resulting from the appearance of open orbits.

The period of the oscillations observed below the helicon threshold depends on H , increasing appreciably with decreasing H . This dependence was first established by Weisbuch and Libchaber^[7] and was later studied in more detail in^[10,12,13]. That the oscillations on curves 2 and 2' are not strictly periodic is quite evident. The results of our measurements of the period as a function of H are shown in Fig. 4. The points on this figure represent the ratio of the observed period ΔH to the calculated period $(\Delta H)_{\text{GK}}$ of the Gantmakher-Kaner oscillations for $p_0 = 0.59 \text{ \AA}^{-1}$. In our experiments the period varied by 40%; this agrees with the results obtained in^[10,12,13].

The experimental values of the phase $k'd$ of the transmitted signal corresponding to the minima of the doppleron oscillations are shown by the points in Fig. 3. The phase was determined in the same way as in^[6]. The experimental points lie close to the theoretical $k'(H)$ curve describing the doppleron spectrum. The scatter of the points on Fig. 4 is due to errors in determining the period of the oscillations on the experimental curves. If we disregard this scatter we see that the H dependence of the period is in good agreement with the theoretical prediction.

The curves on Fig. 5 were obtained at a frequency of 167 kHz. Changing the frequency shifts the entire oscillation pattern along the H axis, the position of the pattern on that axis being proportional to the cube root of the frequency. This shift is the same for both the helicon oscillations and the doppleron oscillations.

Thus, the polarization of the observed oscillations

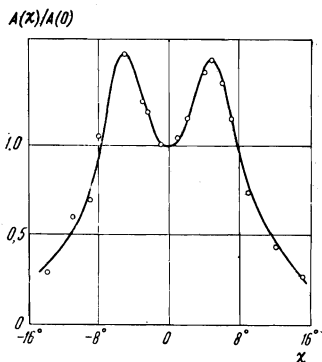


FIG. 6. Amplitude of doppleron oscillations vs magnetic field tilt; $\omega/2\pi = 167$ kHz, $d = 0.25$ mm, $T = 4.2^\circ\text{K}$.

and the behavior of their period are in full agreement with the theoretical predictions derived from our model. In other words, the hypothesis of the existence of a weakly damped electromagnetic wave—the doppleron—leads to a good description of the characteristic properties of the oscillations. We note, however, that there are experimental results that our model cannot account for. These include the dependence of the amplitude of the doppleron oscillations on the angle χ , and the behavior of the impedance in weak fields.

The amplitude A of the doppleron oscillations depends on the angle χ between H and the $[110]$ axis. As χ increases from zero, A increases, reaches a maximum at $\chi \approx 5^\circ$, and then falls off. There are no oscillations at all when $\chi > 20^\circ$. The experimental results on the χ dependence of A are presented in Fig. 6.

Shorter-period oscillations are observed in weak fields ($H < 3$ kOe). A few peaks of such oscillations can be seen on the curves in Fig. 5. Increasing the frequency shifts the short-period oscillations along the H axis, the field strength at which the oscillations appear being proportional to $\omega^{1/3}$. These oscillations are apparently associated with multiple resonances. The presence of such resonances is due to the lack of axial symmetry of the Fermi surface. For a quantitative description of multiple resonances and the associated oscillations one would require a more complicated model than ours, which gives no multiple resonances at all. The multiple resonance problem is beyond the scope of this paper.

The authors are grateful to V. G. Fastovskii for his interest in the work and V. A. Gasparov for providing the pure copper specimens.

¹⁾The single crystal was grown by G. Le-Hirisi (Centre d'études de Chimie Metallurgique, France).

- ¹O. V. Konstantinov and V. I. Perel', Zh. Eksp. Teor. Fiz. 38, 161 (1960) [Sov. Phys.-JETP 11, 117 (1960)].
²V. F. Gantmakher and E. A. Kaner, Zh. Eksp. Teor. Fiz. 48, 1572 (1965) [Sov. Phys.-JETP 21, 1053 (1965)].
³J. C. McGroddy, J. L. Stanford, and E. A. Stern, Phys. Rev. 141, 437 (1966).
⁴A. W. Overhauser and S. Rodriguez, Phys. Rev. 141, 431 (1966).
⁵L. M. Fisher, V. V. Lavrova, V. A. Yudin, O. V. Konstantinov, and V. G. Skobov, Zh. Eksp. Teor. Fiz. 60, 759 (1971); 63, 224 (1972) [Sov. Phys.-JETP 33, 410 (1971); 36, 118 (1973)].
⁶V. V. Lavrova, S. V. Medvedev, V. G. Skobov, L. M. Fisher, and V. A. Yudin, Zh. Eksp. Teor. Fiz. 64, 1839 (1973) [Sov. Phys.-JETP 37, 929 (1973)].
⁷G. Weisbuch and A. Libchaber, Phys. Rev. Lett. 19, 498 (1967).
⁸D. S. Falk, B. Gerson, and J. F. Carolan, Phys. Rev. B1, 406 (1970).
⁹B. G. Chambers and V. G. Skobov, J. Phys. F1, 202 (1971).
¹⁰P. R. Antoniewicz, L. T. Wood, and J. D. Gavenda, Phys. Rev. Lett. 21, 998 (1968).
¹¹P. R. Antoniewicz, Phys. Rev. 185, 863 (1969).
¹²B. Perrin, G. Weisbuch, and A. Libchaber, Phys. Rev. B1, 1501 (1970).
¹³L. T. Wood and J. D. Gavenda, Phys. Rev. B2, 1492 (1970).
¹⁴V. F. Gantmakher, V. A. Gasparov, G. I. Kulesko, and V. N. Matveev, Zh. Eksp. Teor. Fiz. 63, 1752 (1972) [Sov. Phys.-JETP 36, 925 (1973)].

Translated by E. Brunner

74